Received: 24 March 2016 | Revised and accepted: 2 August 2016 | Uncorrected manuscript published: 5 August 2016 | Published on: 3 October 2016

DOI 10.1111/tra.12429

WILEY Traffic

ORIGINAL ARTICLE

Tracking adenovirus genomes identifies morphologically distinct late DNA replication compartments

Tetsuro Komatsu[1,2] | Derrick R. Robinson[1] | Miharu Hisaoka[2] | Shuhei Ueshima[2] | Mitsuru Okuwaki[2] | Kyosuke Nagata[2] | Harald Wodrich[1]

[1]Microbiologie Fondamentale et Pathogénicité, MFP CNRS UMR 5234, Université de Bordeaux, Bordeaux, France

[2]Department of Infection Biology, Faculty of Medicine, University of Tsukuba, Tsukuba, Japan

Corresponding Author: Harald Wodrich, Microbiologie Fondamentale et Pathogénicité, MFP CNRS UMR 5234, Université de Bordeaux, Bordeaux 33076, France (harald.wodrich@u-bordeaux.fr)

In adenoviral virions, the genome is organized into a chromatin-like structure by viral basic core proteins. Consequently viral DNAs must be replicated, chromatinized and packed into progeny virions in infected cells. Although viral DNA replication centers can be visualized by virtue of viral and cellular factors, the spatiotemporal regulation of viral genomes during subsequent steps remains to be elucidated. In this study, we used imaging analyses to examine the fate of adenoviral genomes and to track newly replicated viral DNA as well as replication-related factors. We show de novo formation of a subnuclear domain, which we termed Virus-induced Post-Replication (ViPR) body, that emerges concomitantly with or immediately after disintegration of initial replication centers. Using a nucleoside analogue, we show that viral genomes continue being synthesized in morphologically distinct replication compartments at the periphery of ViPR bodies and are then transported inward. In addition, we identified a nucleolar protein Mybbp1a as a molecular marker for ViPR bodies, which specifically associated with viral core protein VII. In conclusion, our work demonstrates the formation of previously uncharacterized viral DNA replication compartments specific for late phases of infection that produce progeny viral genomes accumulating in ViPR bodies.

KEYWORDS

adenovirus, click chemistry, EdU labeling, Mybbp1a, nucleous, subnuclear structure, ViPR body

1 | INTRODUCTION

DNA viruses that replicate in the nucleus deliver incoming genomes in condensed and transcriptionally inactive form to allow them to be stored during transport. Once delivered to the nucleus, genome condensation needs to be reversed for transcription and replication to commence. In late phases of infection, viral genomes are first amplified, then recondensed and packed into progeny virions for the next round of infection. Several lines of evidence suggest that viral genomes are subjected to dynamic chromatinization with cellular and viral chromatin proteins throughout the different phases of their replication cycle.[1] Like cellular chromatin, the resulting chromatin structure plays a critical role in genome functions, eg, as template for transcription or replication.[1] Additionally, viral genome/chromatin has to be remodeled from an 'intracellular' to an 'intravirion' form to be packed into viral particles before or during virion assembly and maturation. Despite these essential steps, for many DNA viruses, the timing, the mechanistic details and the subcellular environment where these transitions take place remain largely unknown.

Adenovirus (Ad) is a nonenveloped double-stranded DNA virus, with an icosahedral capsid mainly composed of homo-trimers of hexon.[2] Inside the capsid, the linear double-stranded DNA genome forms the chromatin-like structure with basic viral core proteins, protein VII, V and X/mu.[2,3] Protein VII is a 'histone-like' major DNA binding protein and is thought to remain associated with incoming viral DNA at least for several hours after infection,[4,5] although this is still under debate.[3] During the first few hours of infection, the chromatin structure of the viral genome changes. We have shown that cellular histones are deposited onto incoming viral genomes.[5] We also reported that newly replicated viral DNAs associate with cellular histones.[6] Our analyses on histone deposition are consistent with other independent biochemical studies.[7–10] The deposition of cellular

histones onto newly replicated Ad genomes is DNA replication-independent, as indicated by the exclusive binding of histone H3.3, a replication-independent H3 variant.[6] This situation is unlike for the cellular genome where histone deposition is coupled to DNA replication.[11] This conclusion is further supported by the observation that histones are excluded from Ad DNA replication compartments.[6] Using antibodies against the viral single-strand DNA-binding protein (DBP), viral DNA replication compartments can be visualized as round, morphologically distinct structures inside the nucleus.[12] Fluorescence in situ hybridization and BrdU incorporation experiments demonstrated that these structures are bona fide sites for viral DNA replication, and that once synthesized in replication compartments, viral genomes spread into the neighboring areas where viral late transcription takes place.[12] Thus, it was hypothesized that newly replicated viral DNAs become chromatinized with histone H3.3 and serve as templates for viral late gene expression.[6] Additionally, following replication, newly synthesized Ad genomes are incorporated into progeny virions. Since histones are not present in newly assembled virions, they must be removed before viruses leave the cell, or alternatively 'histone-free' genomes have to be selectively synthesized and incorporated into progeny virion. In addition, the deposition of core proteins (eg, protein VII) onto viral genomes is required to form the chromatin-like structures in newly assembled virions. To date, little is known about the site and the viral/cellular factors involved in this unique process. A recent report showed that the cellular ubiquitin specific protease USP7/HAUSP colocalizes with DBP in viral DNA replication centers.[13] Intriguingly, the same report mentioned that USP7 localization also showed morphologically distinct 'ring-like' structures in some cells, although it was not investigated whether this is linked to viral DNA replication.[13] Similar to progeny genome assembly, the spatial organization of Ad capsid/virion assembly is also ill defined. It has been previously shown that L1 52/55K protein is present in assembling immature virions, labels nuclear areas different from replication compartments late in infection, and thus could be a marker of subnuclear territories where virion assembly takes place.[14] In summary, we lack essential knowledge of how virion assembly, viral chromatin assembly and genome packaging are organized in an Ad infected cell.

The nucleolus is one of the most prominent subnuclear structures and plays a central role in many cellular, as well as viral, processes.[15,16] Previously, we have reported that a host nucleolar protein B23.1/Nucleophosmin/NPM1 is associated with both core protein V and the precursor of protein VII (pre-VII) in late phases of infection and may play a role in viral chromatin assembly during progeny virion maturation.[17,18] Ugai et al. recently suggested a potential involvement of B23.1 in viral capsid assembly.[19] In addition to B23.1, other nucleolar proteins are implicated in the Ad infection processes. Matthews and coworkers used proteomic approaches to show that several nucleolar proteins, including Nopp140, are dynamically redistributed in late phases of Ad infection,[20] suggesting that they may participate specifically in the last step(s) of the viral life cycle. Mybbp1a is another regulator of nucleolar processes. Under physiological conditions, Mybbp1a is associated with epigenetic modulators to regulate ribosomal RNA transcription,[21,22] an activity which is correlated with the rate of cellular proliferation, and deletion of the Mybbp1a gene results in embryonic death in mice.[23] Mybbp1a was also shown to regulate the stability of the major tumor suppressor p53 upon nucleolar stress.[24] These findings suggest that Mybbp1a is an important factor in multiple nucleolar/cellular mechanisms. However, the involvement of Mybbp1a in Ad infection has not been investigated.

In this study, we used direct DNA labeling and imaging techniques to investigate the fate of newly replicated viral genomes as well as changes of viral DNA replication compartments during late phases of infection, at a time when chromatinization and packaging of progeny genomes is likely to take place. Our analysis suggests that Ad DNA replication is organized into early and late replication compartments. We identify the latter by showing the de novo formation of a subnuclear domain, which we have termed Virus-induced Post-Replication (ViPR) body, which forms in the center of late replication compartments and serves as a receiving reservoir for newly replicated viral genomes. We also show specific recruitment of the nucleolar protein Mybbp1a into ViPR bodies and discuss the potential implications for viral genomes during progeny virion maturation.

2 | RESULTS

2.1 | 'Late' structures emerge after 'early' Ad DNA replication compartments disappear

First, to confirm the previous observations of USP7 behavior during Ad infection,[13] we carried out immunofluorescence (IF) analyses on cells infected with Ad type 5 (Ad5) using antibodies against DBP and USP7 (Figure 1A). In uninfected cells, USP7 was observed throughout the nucleus with small dot-like structures (Figure 1A, first row). At 12 hours postinfection (hpi) USP7 either remained diffusely localized (Figure 1A, second row) or showed numerous dots that were colocalized with DBP (Figure 1A, third row). At 24 hpi, USP7 either localized at previously described DNA replication compartments marked by DBP (Figure 1A, fourth row) or exhibited the 'ring-like' structures described previously[13] (Figure 1A, fifth row). Our analysis also revealed that DBP translocated into the same 'ring-like' structures together with USP7 (Figure 1A, fifth row), suggesting a potential role of the structures in viral DNA replication (see below). Importantly, no coexistence of the two structures in one cell was observed: if a cell had the classical replication compartments, the 'ring-like' structures were absent, and vice versa. Analogous results were obtained in other cell lines (Figure 1B, H1299), excluding a cell type-specific observation. Next we examined the relocalization of USP7 during Ad infection in more detail. We categorized the localization patterns into four groups (i–iv, shown in Figure 1A) and quantified their appearance over time using IF analyses (Figure 1C). In agreement with a recent report,[13] the category i (diffuse) and ii (dot-like) USP7 localization gradually decreased over time. In contrast, our quantification indicated that category iii (classical replication compartments) was first increased (approximately 50% at 16 and 20 hpi) and then decreased (22.7% at 24 hpi) over time, whereas category iv (the 'ring-like' structures) was gradually increased as infection progressed (23.4% at 20 hpi and 70.9% at 24 hpi). Taken together, these results suggest that in late phases of infection, the classical DNA replication compartments were first formed but then disintegrated or

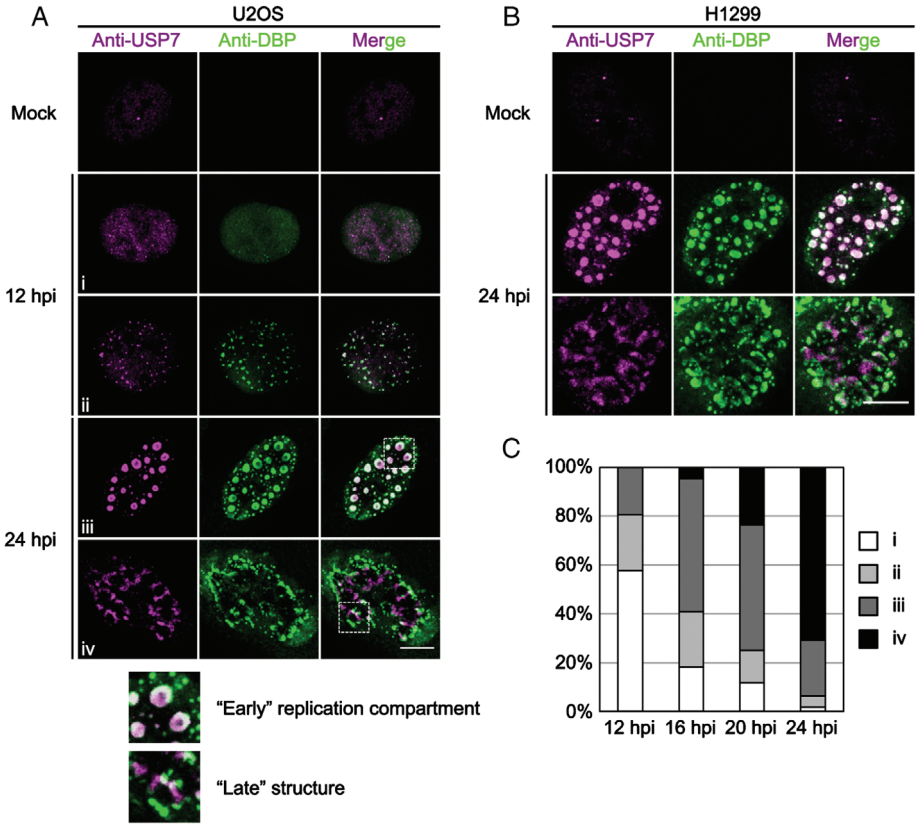

FIGURE 1 Late phase-specific subnuclear structures in adenovirus (Ad)-infected cells. (A) Immunofluorescence (IF) analyses with anti-USP7 antibody. U2OS cells were either mock-infected or infected with Ad5 and at 12 and 24 hours postinfection (hpi) subjected to IF analyses using indicated antibodies. Merged images are shown in the third column. Higher-magnified images of the regions marked by squares are shown in lower panels as representatives for the early replication compartments and the late structures. (B) IF analyses with H1299 cells. H1299 cells were subjected to IF analyses using indicated antibodies at 24 hpi. (C) Time–course analyses of USP7 localization. The localization patterns of USP7 in infected cells were divided into four groups (i–iv, shown in A). IF samples were prepared at 12, 16, 20 and 24 hpi. For each time-point, cells showing each localization pattern were counted, and the population was graphed with the percentage (n = 109, 127, 128 and 110 for 12, 16, 20 and 24 hpi, respectively).

transformed concomitantly with emerging of the 'ring-like' structures. Because both structures are marked by the same proteins and exhibit a somewhat 'round' phenotype (although being clearly morphologically distinct), for the sake of clarity, we decided hereafter to name these structures based on the timing of their appearance in the infection cycle: 'early replication compartments' (ie, category iii structures) and 'late structures (ie, category iv structures or late replication compartments, see below)', as indicated in Figure 1A.

2.2 | Nucleolar protein Mybbp1a accumulates in the center of the late structures

We next sought to further gain insights into how the late structures are formed during Ad infection. We hypothesized that nucleolar proteins might be reorganized at this time (see *Introduction* section). To test this, we examined the localization of three nucleolar proteins, B23.1, Nopp140 and Mybbp1a, in infected cells using transiently expressed EGFP-FLAG (EF) or EGFP-3×FLAG (E3F) tagged proteins (Figure 2A). At 24 hpi, the localization of USP7 was either in the early replication compartments (Figure 2A, second row) or the late structures (Figure 2A, third row) in the majority of cells, as described above. In mock-infected cells, all of EGFP-tagged nucleolar proteins tested were localized in nucleoli (Figure 2A, first row). Consistent with our previous study,[17] the localization of EF-B23.1 was almost unchanged upon Ad infection under our experimental conditions (Figure 2A, first column), although relocalization of the protein was previously reported by others.[25] EF-Nopp140 showed smaller punctate signals at 24 hpi (Figure 2A, third column), which were partially overlapping with the early replication compartments (second row) and the late structures (third row) shown in the panels stained for USP7. In sharp contrast, relocalization of E3F-Mybbp1a was observed only in cells showing the late structures (Figure 2A, fifth column, third row), but not the early replication compartments (second row), and this protein showed exclusive localization in the center of the late structures delineated by either USP7 or DBP (Figure 2A, Merge). The recruitment of E3F-Mybbp1a into the late structures was also observed in H1299 cells (Figure S1A, Supporting Information), suggesting that this is not cell type-specific. We also confirmed that transiently expressed FLAG-tagged Mybbp1a was recruited into the late structures (Figure S1B), excluding the effect of the large tag (EGFP-3×FLAG). Therefore, these results indicate that Mybbp1a selectively accumulates in the center of the late structures when they are present and that this recruitment is unlikely to be a general feature of nucleolar proteins.

To confirm the specific translocation of Mybbp1a, we examined the localization of Mybbp1a and B23.1 in the same cells using different tags (Figure 2B). In mock-infected cells, both E3F-Mybbp1a and DsRed1-B23.1 remained confined to nucleoli (Figure 2B, first row). Likewise, at 24 hpi, both proteins remained colocalized in nucleoli in cells still displaying the early replication compartments (Figure 2B, second row). However, we observed specific accumulation of E3F-Mybbp1a into the center of the late structures (Figure 2B, third row), while DsRed1-B23.1 remained confined to nucleoli in these cells. This result strongly supports the idea that Mybbp1a is specifically recruited out of nucleoli and toward the center of the late structures.

Next, we wanted to follow this translocation dynamically. To this end, we carried out live-cell imaging analyses to examine how Mybbp1a is dynamically relocalized upon Ad infection (Figure 2C and Movie S1). U2OS cells transiently expressing low levels of E3F-Mybbp1a were infected with Ad5 and subjected to live-cell imaging from 17 to 25 hpi; the late structures started to form around 16 hpi

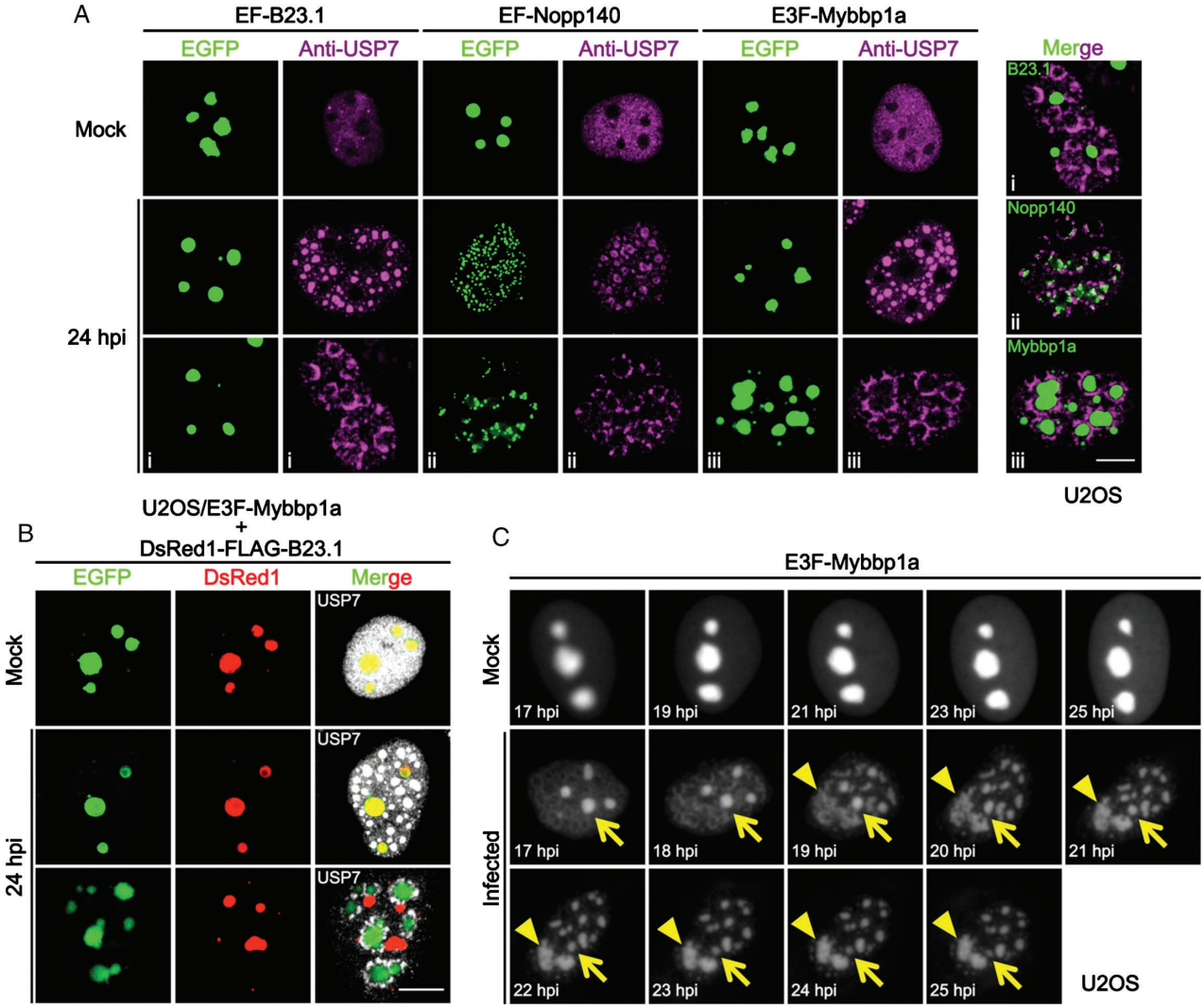

FIGURE 2 Mybbp1a localizes inside the late structures. (A) Localization of EGFP-tagged nucleolar proteins in adenovirus (Ad)-infected cells. U2OS cells transiently expressing EGFP-tagged B23.1, Nopp140 or Mybbp1a were either mock-infected or infected with Ad5 and at 24 hours postinfection (hpi) subjected to immunofluorescence (IF) analyses using anti-USP7 antibody. For the images in third row, merged images are shown in the seventh column (i, ii and iii for B23.1, Nopp140 and Mybbp1a, respectively). (B) Localization of EGFP-tagged Mybbp1a and DsRed1-tagged B23.1 in infected cells. U2OS/E3F-Mybbp1a cells transiently expressing DsRed1-FLAG-B23.1 were infected with Ad5 and at 24 hpi subjected to IF analyses using anti-USP7 antibody. Merged images of EGFP, DsRed1 and USP7 localization (gray) are shown in the third column. (C) Time-lapse analyses of E3F-Mybbp1a localization in infected cells. U2OS cells expressing E3F-Mybbp1a were infected with Ad5, and live-cell imaging was started at 17 hpi. Series of snapshots are shown (every 2 hours for mock and every 1 hour for infected cells). Arrows and arrowheads indicate preexisting nucleoli and newly forming bodies, respectively. Full movies are provided as Movie S1.

in some cells (Figure 1C). At 17 hpi, E3F-Mybbp1a predominantly localized in nucleoli. However, the nucleolar signals decreased over time (Figure 2C, indicated by arrows) while new Mybbp1a-containing domains, constantly increasing in size, formed outside nucleoli (Figure 2C, indicated by arrowheads). These results confirmed that the emerging subnuclear compartments containing E3F-Mybbp1a were formed de novo at the inside of the late structures, rather than resulting from the movement of preexisting nucleoli.

We next tried to observe endogenous Mybbp1a in infected cells using specific antibodies. Under our experimental conditions, however, we could not detect endogenous Mybbp1a in IF analyses (Figure 3A, second column). Only transiently expressed E3F-Mybbp1a could be detected (Figure 3A, fourth column), suggesting that the antibody is functional and that endogenous Mybbp1a levels are too low to be detected. To not rely on transient transfection, we decided to prepare a cell line stably expressing E3F-Mybbp1a for further analyses (hereafter U2OS/E3F-Mybbp1a cells). Importantly, the stable expression of exogenous E3F-Mybbp1a altered the morphology of neither the early replication compartments nor the late structures when compared to control cells (data not shown, see below). Furthermore, we confirmed that the expression of E3F-Mybbp1a affected neither viral DNA (Figure 3B) nor protein levels (see Figure 6D, lanes 1–4), validating our approach of using stable expression of exogenous Mybbp1a.

2.3 | Late structures are associated with viral DNA synthesis activity

USP7, together with DBP, marked not only the late structures but also the early replication compartments (Figure 1), suggesting some

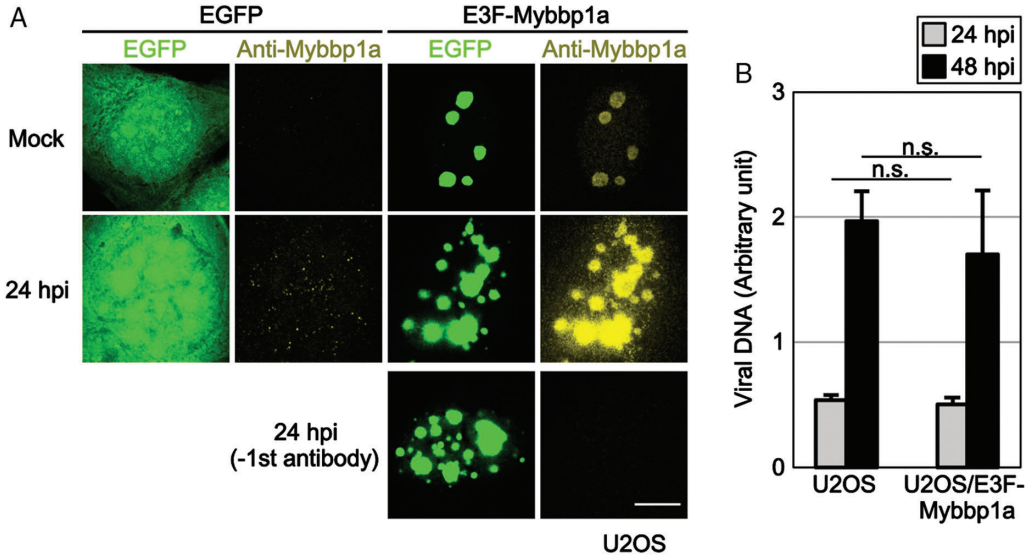

FIGURE 3 Overexpression of E3F-Mybbp1a does not affect adenovirus (Ad) infection processes. (A) Immunofluorescence (IF) analyses with anti-Mybbp1a antibody. U2OS cells transiently expressing either EGFP alone or E3F-Mybbp1a (green) were infected with Ad5, and at 24 hours postinfection (hpi) IF samples were prepared with (first and second rows) or without (third row) anti-Mybbp1a antibody (yellow). (B) Effect of Mybbp1a overexpression on viral DNA amounts. Control U2OS or U2OS cells stably expressing E3F-Mybbp1a (U2OS/E3F-Mybbp1a) were infected with Ad5 and collected at 24 and 48 hpi for the extraction of viral DNAs. Viral DNA amounts were quantified by qPCR using the primer set for the hexon gene. qPCRs were performed in triplicate and error bars represent SD in one experiment. *P*-values were calculated using Student's *t*-test. 'n.s.' indicates 'not statistically significant'. Two independent experiments showed similar results.

kind of functional relationship. Therefore we wanted to determine whether the late structures also participate in viral DNA replication. To directly visualize viral DNA replication activities and newly replicated viral genomes, 5-ethynyl-2′-deoxyuridine (EdU) labeling assays were carried out (Figure 4).[26] First we examined whether EdU can be incorporated into viral DNA under our experimental conditions. EdU was added to the culture medium at 23 hpi, and after 1-h incubation, cells were collected for EdU detection, followed by IF analyses (Figure 4A). In cells showing the early replication compartments, EdU signals were overlapping with USP7 and DBP localization (Figure 4A, second row, also see Merge), indicating that EdU can be a substrate for Ad DNA replication and is specifically incorporated into viral replication compartments. Next, we performed the same analyses using U2OS/E3F-Mybbp1a cells (Figure 4B). In this case, E3F-Mybbp1a was detected using anti-Mybbp1a antibody, as the fluorescence of EGFP is lost during click chemistry. In infected cells showing the early replication compartments, Mybbp1a remained localized in nucleoli (indicated by lack of DAPI staining) and did not overlap with EdU signals, which accumulated in the early replication compartments (Figure 4B, second row, arrowheads for Mybbp1a and arrows for EdU signals). In contrast, in cells showing relocalized Mybbp1a, EdU was detected depicting the late structures surrounding the Mybbp1a localization, similar to what was observed for USP7 (Figure 4B, third row). These results suggest that viral DNA replication takes place not only in the early replication compartments but also in the late structures. Thus, we identified the late structures formed by USP7 as functional 'late replication compartments'. This conclusion is further supported by the observation that the viral DNA replication factor DBP was also incorporated into the late replication compartments where it partially overlapped with USP7 (Figure 1A and B).

2.4 | Newly synthesized viral genomes move progressively toward the inside of the late replication compartments

We noted that translocated Mybbp1a colocalized with areas that showed strong DAPI staining, which also located inside of the late replication compartments (Figure 4B, third row, arrowheads). EdU signals on the contrary did not overlap with DAPI-stained areas (Figure 4B, third row, arrows). This is consistent with the fact that the early replication compartments are poorly stained by DAPI probably due to abundant single-stranded DNA intermediates (Figure 4B, second row, arrows). Thus, the strong DAPI staining could reflect either cellular chromatin or the accumulation of double-stranded viral genomes. In the latter case, they should be first synthesized at surrounding areas (the late replication compartments marked by USP7 and/or EdU) and then move toward the inside where Mybbp1a is localized. To test this possibility, we performed pulse-chase experiments using EdU (Figure 5). To examine whether viral genome movements previously observed with BrdU pulse labeling[12] can be reproduced using EdU, we first carried out pulse-labeling analyses focusing on the early replication compartments (Figure 5A). EdU was added to the cells at 15 hpi for pulse labeling, and at 16 hpi cells were extensively washed with medium to remove unincorporated EdU and then cultured in the absence of EdU for 2 or 4 h for chasing. Consistent with the results shown above, clear overlapping between EdU signals and USP7 localization in the early replication compartments was observed at 16 hpi (Figure 5A, first row). In contrast, after 2 h of chasing (at 18 hpi), EdU signals were detected mainly at the rim or the outside of the early replication compartments only partially overlapping with USP7 (Figure 5A, second row). This was even more evident at 20 hpi (after 4 h of chasing), as less or no overlap between USP7 and EdU signals

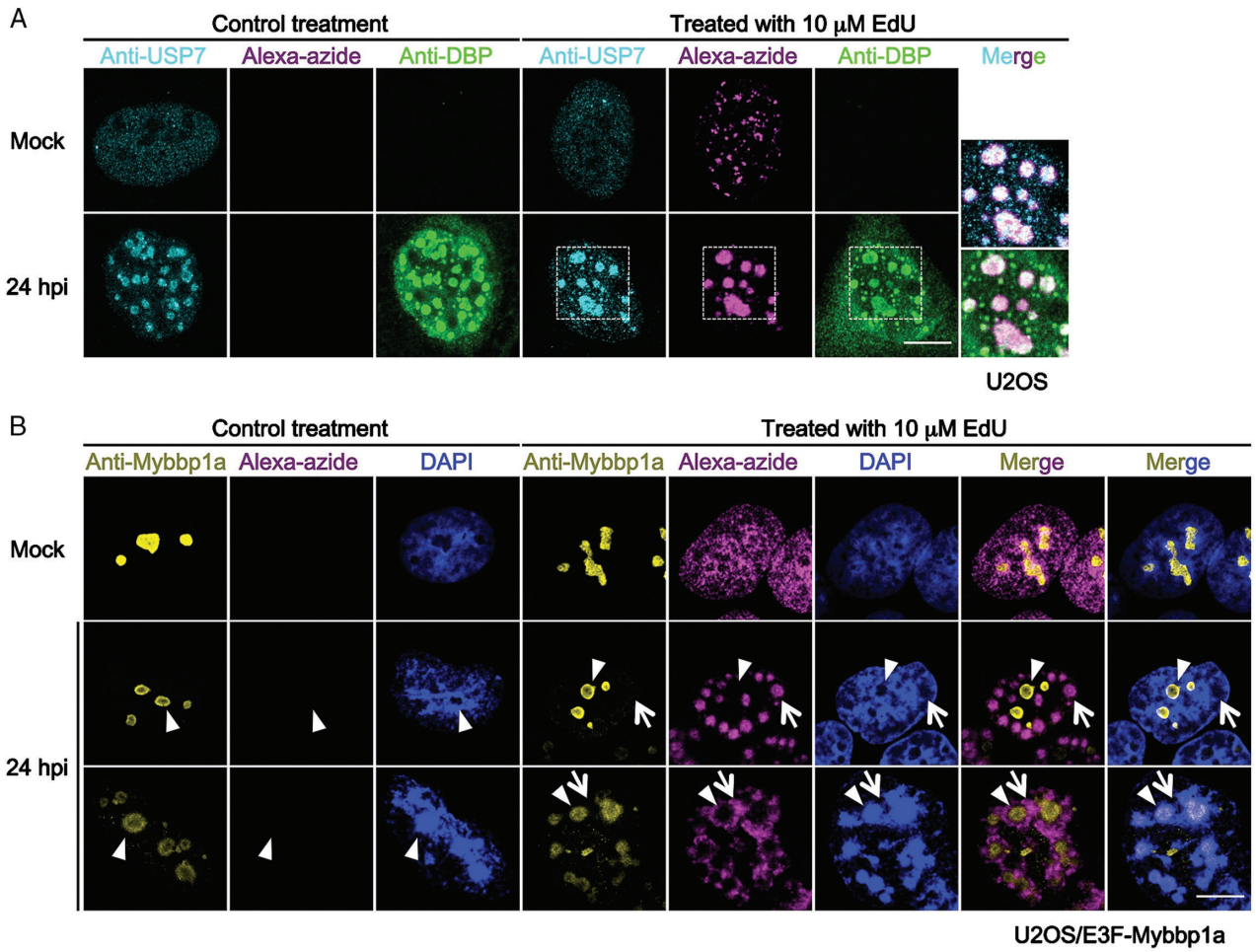

FIGURE 4 The late structures are sites of viral DNA replication. (A) 5-Ethynyl-2′-deoxyuridine (EdU) labeling of newly synthesized viral DNA. U2OS cells were infected with adenovirus type 5 (Ad5), and at 23 hours postinfection (hpi) the culture medium was replaced by either the fresh DMEM (control treatment) or DMEM containing 10 μM EdU (treated with 10 μM EdU). Cell were fixed at 24 hpi and subjected to the Click-iT reaction with alexa-azide, followed by immunofluorescence (IF) analyses using anti-USP7 and anti-DNA-binding protein (anti-DBP) antibodies. Higher-magnified merged images of the regions marked by squares are shown in the seventh column. (B) EdU labeling with U2OS/E3F-Mybbp1a cells. U2OS/E3F-Mybbp1a cells were subjected to EdU labeling analyses with alexa-azide as described above, but using anti-Mybbp1a antibody for IF analyses. DAPI staining is shown in blue. For cells treated with EdU, merged images are shown in the seventh and eighth columns. Arrows and arrowheads indicate EdU signals and Mybbp1a localization, respectively.

was observed (Figure 5A, third row, also see the magnified view below). In summary, we were able to track the movement of viral DNA from the inside to the outside of the early replication compartments by EdU labeling analyses, as previously shown by BrdU labeling.[12]

We next carried out the same analyses focusing on the newly identified late replication compartments using U2OS/E3F-Mybbp1a cells (Figure 5B). EdU was added at 19 hpi, and cells were collected at 20, 22 and 24 hpi. Immediately after labeling (at 20 hpi), EdU signals accumulated depicting the late replication compartments, and no colocalization with Mybbp1a was observed (Figure 5B, first row). At 22 hpi, EdU signals remained partially in the late replication compartments but had also partially associated with the outer region of the Mybbp1a localization (Figure 5B, second row). At 24 hpi, the EdU signal had almost completely moved into the inside of the late replication compartments, showing full overlap with Mybbp1a (Figure 5B, third row, also see the magnified view below). These results using EdU pulse-labeling analyses strongly suggest that late in infection viral DNA is first synthesized at the late replication compartments and then progressively moves toward the inside of the structures marked by Mybbp1a. To the best of our knowledge, the accumulation of newly replicated Ad genomes into specific compartments (ie, the inside of the late replication compartments) has not been reported, and thus our analysis has revealed a novel intranuclear trafficking pattern of replicated viral DNA that takes place in cells at late time-points of infection (>20 hpi under our experimental conditions). These novel subnuclear domains form de novo upon Ad infection, and newly replicated viral genomes are relocalized from DNA replication compartments into these domains. Based on these phenotypic characteristics, we termed this novel domain 'ViPR body'. ViPR bodies are spatially linked to the late replication compartments, but themselves do not show active DNA replication activities (eg, see Figure 4B). Hence, 'the late replication compartments' and 'ViPR bodies' are juxtaposed but distinct structures and indicate only the outer (marked by fresh EdU label, USP7 and DBP) and inner regions (marked by chased EdU label and Mybbp1a), respectively.

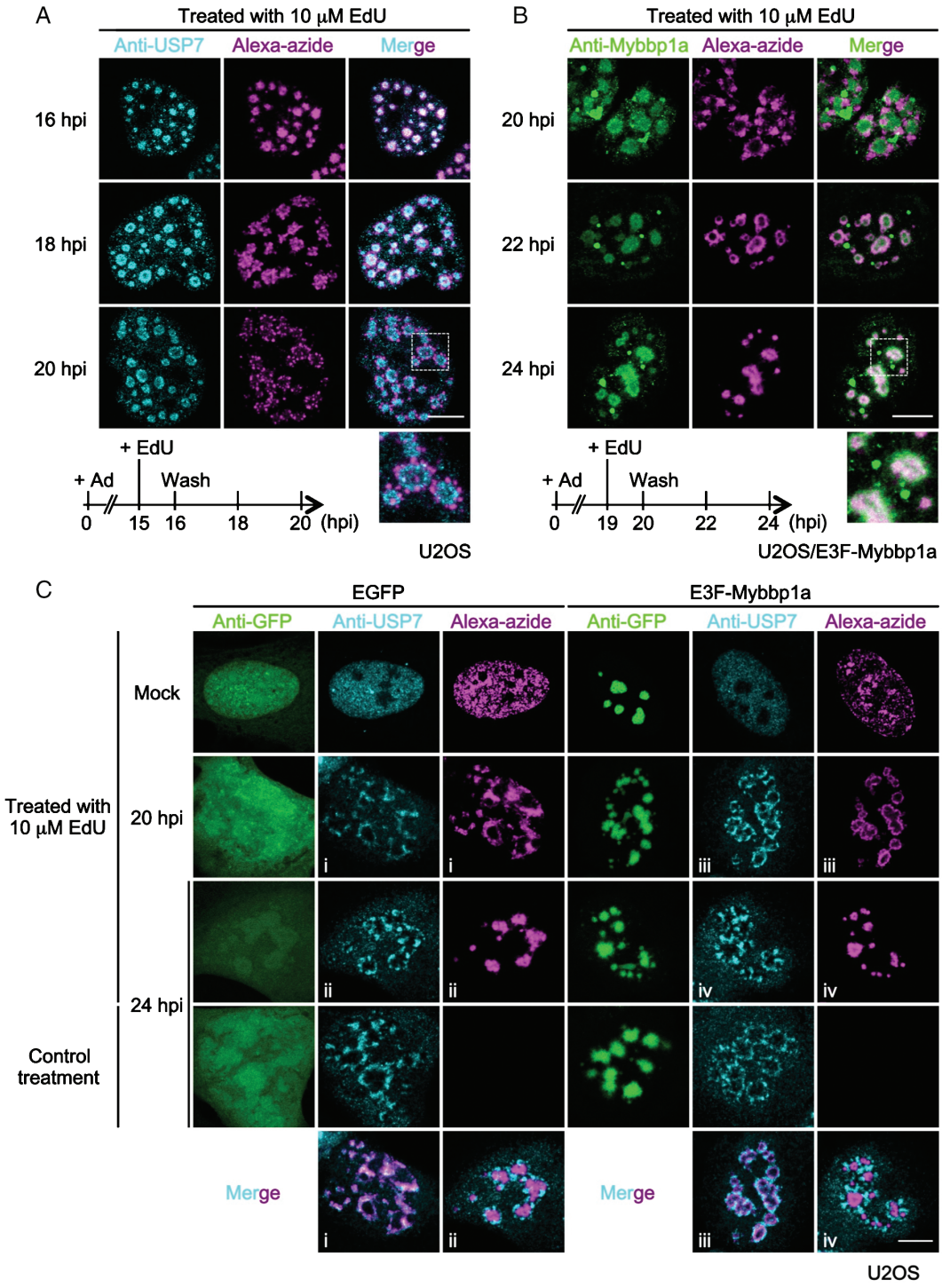

FIGURE 5 Newly synthesized viral DNAs translocate into the inside of the late structures. (A) 5-Ethynyl-2′-deoxyuridine (EdU) pulse-chase analyses. U2OS cells were infected with adenovirus type 5 (Ad5), and at 15 hours postinfection (hpi) the culture medium was replaced by DMEM containing 10 μM EdU. After 1-hour incubation for pulse labeling, cell were washed with DMEM and cultured in the absence of EdU for chasing. At 16, 18 and 20 hpi, cells were fixed and subjected to the Click-iT reaction and immunofluorescence (IF) analyses. Lower panel shows the experimental scheme. (B) EdU pulse-chase analyses with U2OS/E3F-Mybbp1a cells. U2OS/E3F-Mybbp1a cells were infected with Ad5, and 10 μM EdU was added at 19 hpi. After pulse labeling for 1 hour, cells were collected at 20, 22 and 24 hpi for Click-iT and IF. (C) EdU pulse-chase analyses with or without Mybbp1a overexpression. U2OS cells transiently expressing either EGFP alone or E3F-Mybbp1a were subjected to Ad infection and EdU pulse chasing as described in panel (B). The fourth row shows cells without EdU treatment. For the panels i–iv, merged images are shown in the fifth row.

We have shown the formation of ViPR bodies using cells expressing EGFP-tagged Mybbp1a (U2OS/E3F-Mybbp1a). It remained possible that our observations were caused by the exogenous expression of Mybbp1a, although the late replication compartments were observed without overexpression of any exogenous proteins (Figure 1), making it unlikely that exogenous expression of the protein influenced their formation. To exclude the possibility that the accumulation of EdU-labeled viral DNAs was triggered by exogenous

Mybbp1a expression, we repeated the EdU pulse-chase experiments using cells transiently expressing EGFP alone or E3F-Mybbp1a (Figure 5C). In this case, EGFP proteins were detected using a fluorescently labeled anti-GFP antibody. Both in the absence (Figure 5C, EGFP) and presence of overexpressed Mybbp1a (E3F-Mybbp1a), EdU signals were overlapping with the late replication compartments shown by USP7 localization immediately after labeling (at 20 hpi, second row, also see merged images i and iii below) and were detected at the inside after chasing (24 hpi, third row, also see merged images ii and iv below). These results strongly suggest that the formation of ViPR bodies do not require Mybbp1a overexpression and rather take place in a natural context of the Ad infection. In turn, it validates the observation that tagged Mybbp1a can be used as a marker to visualize ViPR bodies without affecting the infection processes as such.

2.5 | Viral core protein VII is associated with Mybbp1a and localizes inside ViPR bodies

We next sought to investigate functions of ViPR bodies and/or Mybbp1a in Ad infection. First, we investigated the relationship between ViPR bodies and capsid/virion assembly. However, when we costained for L1 52/55K, a potential marker for progeny virion assembly (see *Introduction* section),[14] its subnuclear localization was completely excluded from ViPR bodies (Figure S2A). This result suggests that ViPR bodies are unlikely to be compartments where capsid/virion assembly takes place.

We next examined the potential involvement of ViPR bodies in progeny genome assembly with viral core proteins. First, we examined the localization of protein VII and cellular histones in infected cells displaying ViPR bodies by using histone H2B tagged with the fluorescent protein (tdiRFP) (Figure 6A). In cells showing ViPR bodies marked by E3F-Mybbp1a, tagged histone H2B was clearly excluded from the domains (Figure 6A, Merge). Histone exclusion from ViPR bodies was also observed using antibodies against endogenous histone H3 (Figure 6B) and H4 (Figure S2B) or using EGFP-tagged and mCherry-tagged histone H3.3 (T.K., H.W., unpublished data). In contrast to cellular histones, the localization of protein VII partially overlapped with ViPR bodies, showing protein VII enrichment in these structures (Figure 6A, Merge). This localization of protein VII was also observed without Mybbp1a overexpression or EdU labeling and partially overlapped with DAPI-stained areas reminiscent of ViPR bodies (Figure 6C). In contrast, in cells showing the early replication compartments, we could observe neither enrichment nor exclusion of protein VII (Figure S2C). Thus our results show that protein VII is specifically enriched in ViPR bodies while cellular histones are excluded.

We next investigated a potential involvement of Mybbp1a in the regulation of protein VII using biochemical analysis (Figure 6D). U2OS and U2OS/E3F-Mybbp1a cells were infected with Ad5 and subjected to immunoprecipitation using anti-GFP beads (GFP-trap). We observed that protein VII (and/or pre-VII) was coprecipitated with E3F-Mybbp1a (Figure 6D, protein VII, lane 8). This interaction was specific because the major capsid protein hexon was not coprecipitated under the same conditions (Figure 6D, hexon). Intriguingly, coprecipitation of TAF-I, a host protein previously shown to be associated with pre-VII in late phases of infection,[27] was also not observed, suggesting that the interaction between Mybbp1a and protein VII is independent of TAF-I. To further explore the association between Mybbp1a and protein VII, we examined whether endogenous Mybbp1a can interact with protein VII independently of an ongoing viral infection by using transiently expressed EGFP-FLAG-tagged protein VII (Figure 6E). Endogenous Mybbp1a was found coprecipitated with EGFP-FLAG-protein VII but not EGFP alone (Figure 6E, lanes 3 and 4). This suggests that the endogenous protein can interact with protein VII in the absence of any other viral factor(s) including viral DNA, although it remains to be determined whether this interaction is direct or requires additional cellular factors.

Finally, we examined the interaction between Mybbp1a and protein VII using in situ proximity ligation assays (PLA; Figure 6F), a method suitable for the detection of in cellulo interaction of proteins. U2OS cells transiently expressing E3F-Mybbp1a were infected with Ad5 and at 24 hpi subjected to in situ PLA using antibodies against Mybbp1a and protein VII. For the analysis, we selected pairs of transfected and untransfected cells for imaging (Figure 6F, left panel, indicated by arrows and arrowheads respectively) to directly compare these cells under the identical conditions (also see *Materials and methods* section). In uninfected cells, PLA signals were hardly detected regardless of the presence of E3F-Mybbp1a, validating our experimental conditions. At 24 hpi, PLA signals were exclusively observed within the nuclei and detected even in the absence of E3F-Mybbp1a (Figure 6F, left panel), which could reflect the interaction between protein VII and endogenous Mybbp1a. However, the number of nuclear PLA puncta was significantly increased by transient expression of E3F-Mybbp1a (Figure 6F, right panel), in good agreement with IP experiments using E3F-Mybbp1a (Figure 6D). Taken together, these biochemical and microscopic experiments strongly indicate a specific association between Mybbp1a and the major core protein VII during late phases of Ad infection.

3 | DISCUSSION

In this study, we identified morphologically distinct late replication compartments that form after the disintegration of the early replication compartments (>20 hpi under our experimental conditions) (Figure 7A). These late replication compartments surround a novel subnuclear domain, ViPR body, which emerges in late phases of the Ad infection cycle in parallel with the late replication compartments. By tracking newly replicated viral genomes from the late replication compartments, we show that ViPR bodies function as a receiving reservoir for those viral genomes. We also show that ViPR bodies can be morphologically tracked and identified via specific accumulation of the nucleolar protein Mybbp1a.

In infected cells, cellular histones are deposited onto incoming as well as newly replicated viral genomes. However, since histones are not present in Ad particles, they must be either removed before packaging or alternatively not be deposited onto viral genomes used for incorporation into progeny virions in the first place. Our previous study revealed that cellular histones are excluded from the early replication compartments, and that histone H3.3 is deposited onto the

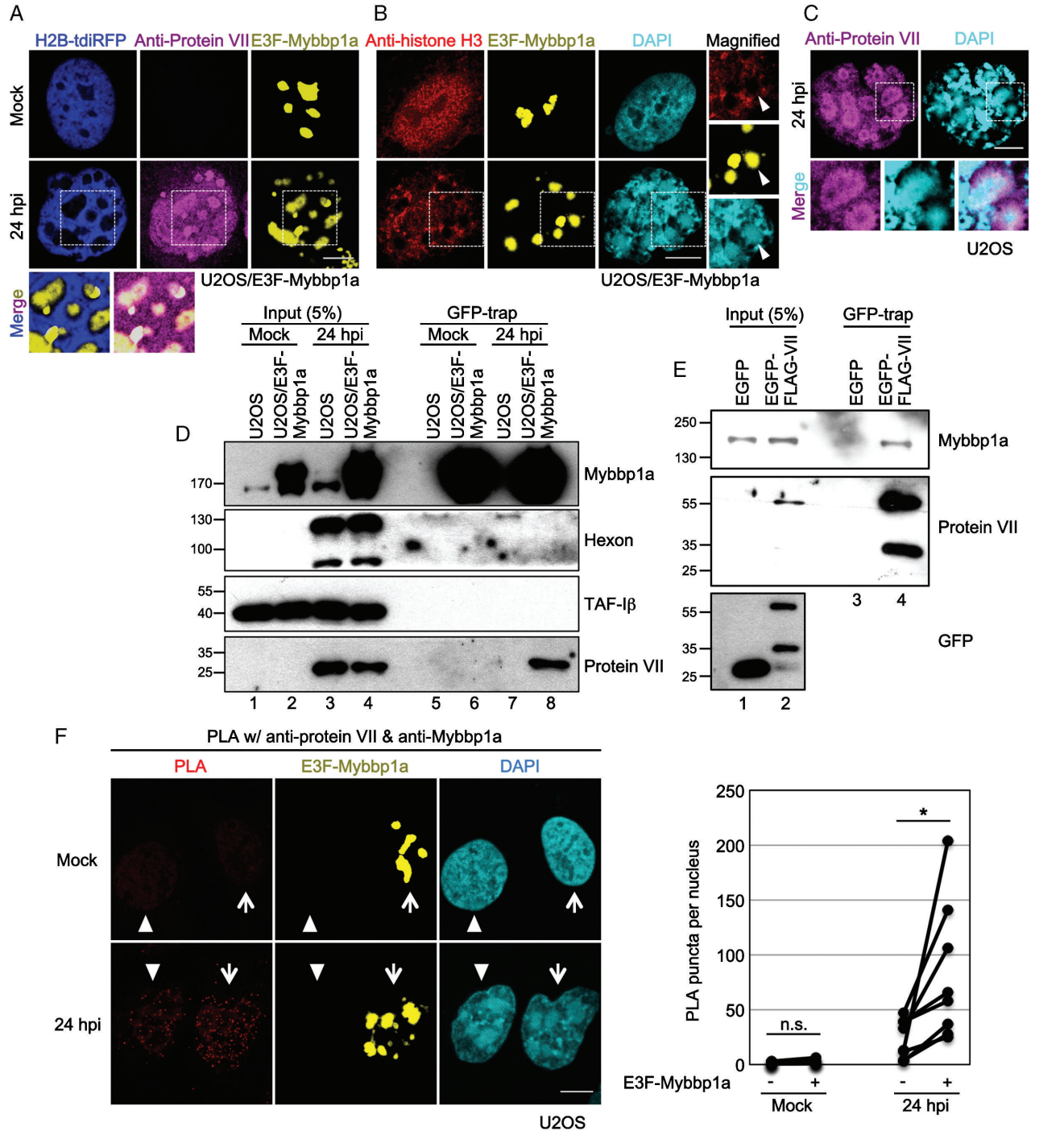

FIGURE 6 Viral core protein VII interacts with Mybbp1a and localizes to ViPR bodies. (A) Immunofluorescence (IF) analyses with histone H2B-tdiRFP and anti-protein VII antibody. U2OS/E3F-Mybbp1a cells transiently expressing histone H2B-tdiRFP were infected with adenovirus type 5 (Ad5), and at 24 hours postinfection (hpi) IF samples were prepared using anti-protein VII antibody. (B) IF analyses using anti-histone H3 antibody. U2OS/E3F-Mybbp1a cells were infected with Ad5 and at 24 hpi subjected to IF analyses using anti-histone H3 antibody. DAPI staining is shown in cyan. (C) IF analyses anti-protein VII antibody. U2OS cells were infected with Ad5 and at 24 hpi subjected to IF analyses using anti-protein VII antibody. (D) IP analyses using anti-GFP beads. U2OS (lanes 1, 3, 5 and 7) or U2OS/E3F-Mybbp1a cells (lanes 2, 4, 6 and 8) were either mock-infected (lanes 1, 2, 5 and 6) or infected with Ad5 (lanes 3, 4, 7 and 8). At 24 hpi, cell lysates were prepared and subjected to immunoprecipitation using anti-GFP agarose beads (GFP-trap). 5% of lysates (lanes 1–4) and precipitates (lanes 5–8) were subjected to SDS–PAGE, followed by western blot analyses using indicated antibodies. (E) IP analyses with EGFP-FLAG-protein VII. U2OS cells transiently expressing either EGFP alone (lanes 1 and 3) or EGFP-FLAG-protein VII (lanes 2 and 4) were subjected to GFP-trap. 5% of lysates (lanes 1 and 2) and precipitates (lanes 3 and 4) were subjected to SDS–PAGE, followed by western blot analyses using indicated antibodies. (F) In situ PLA with anti-protein VII and anti-Mybbp1a antibodies. U2OS cells transiently expressing E3F-Mybbp1a were infected and at 24 hpi subjected to in situ PLA using antibodies against protein VII and Mybbp1a. Pairs of transfected and untransfected cells (indicated by arrows and arrowheads respectively) were selected and imaged (left panel, also see *Materials and methods* section). PLA puncta per nucleus were counted, and *P*-values were calculated using paired *t*-test (right panel, $n = 8$, $^*P < 0.05$).

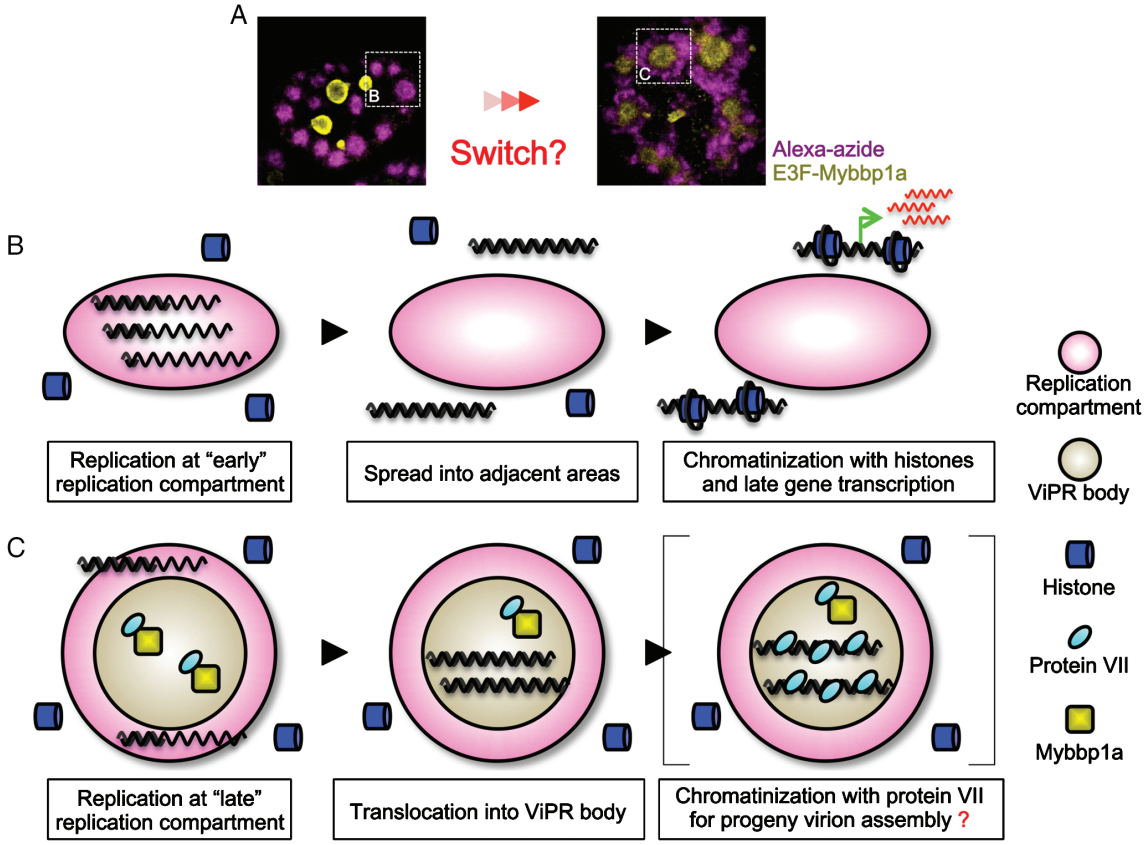

FIGURE 7 A model for subnuclear trafficking of adenovirus (Ad) genomes in late phases of infection. (A) Two different subnuclear structures in late phases of Ad infection. The early replication compartments emerge first (left panel) but then disintegrate concomitantly with the formation of the late replication compartments and ViPR bodies (right panel). A switching mechanism(s) is currently unknown. Images are taken from Figure 4B. The regions marked by squares are schematically illustrated below. (B) The early replication compartment. Ad genomes are synthesized at the early replication compartments. Viral DNAs spread into the neighboring nucleoplasmic areas and then are subjected to histone deposition. Viral genomes chromatinized with histones function as templates for late gene expression (viral transcription and transcripts are shown in green and red, respectively). (C) The late replication compartment and Virus-induced Post-Replication (ViPR) body. Viral genomes are synthesized at the late replication compartments surrounding ViPR bodies where Mybbp1a interacts with protein VII. Replicated viral DNAs then move progressively toward ViPR bodies. Thus, ViPR bodies may be involved in chromatinization of viral genomes for progeny virions. For details, see *Discussion* section.

viral chromatin in a replication-uncoupled manner.[6] Based on this, we proposed a model that replicated, but 'histone-free' genomes spread from the early replication compartments into the adjacent areas, where cellular histones are localized, and then genomes are chromatinized with histone H3.3 to be templates for viral late gene expression (Figure 7B).[6] Here we provide evidence that viral DNAs synthesized at the late replication compartments move into ViPR bodies where the viral core protein VII but not cellular histones are present (Figure 7C). Therefore, it is reasonable to speculate that ViPR bodies play a role in the organization of viral genomes prior to packaging into progeny virions. Our findings thus suggest the existence of different types of replicated genomes and a spatial and temporal compartmentalization (early replication compartment-derived for transcription predominating at 16–20 hpi vs late replication compartment-derived potentially for progeny virion incorporation predominating from 20 hpi onward), which may allow specific chromatinization pathways and would provide a rationale for the absence of histones in virions.

We showed that Mybbp1a and protein VII specifically interact, suggesting a functional link. We previously showed that newly replicated viral genomes are occupied by the chromatin-organizing factor CTCF,[28] (CCCTC-binding factor) which is reported to interact with Mybbp1a.[29] In addition, proteomic studies and biochemical analyses have identified several chromatin modulators as interactors of Mybbp1a.[21,22,29,30] Taken together, this raises the possibility that Mybbp1a may be part of a chromatin-remodeling complex, which controls viral chromatin assembly linked to genome organization and/or incorporation into progeny virions. However, further studies are needed to assert and understand the role (if any) of Mybbp1a in late viral chromatin assembly. Although we performed Mybbp1a knockdown experiments, the knockdown resulted in decreased levels of viral DNA and protein production, which precedes the appearance of ViPR bodies (T.K., H.W., unpublished observation). This impedes examining the role(s) of Mybbp1a in ViPR bodies using depletion approaches. It would be interesting for future studies to test if the localization of protein VII in ViPR bodies is dependent on Mybbp1a. Another important question that remains to be investigated is to identify what triggers the drastic morphological changes between early and late replication compartments, leading to the formation of ViPR bodies (Figure 7A).

Despite these open questions, there are some similarities with other viral systems. For instance, it was shown that genomes of human cytomegalovirus (HCMV) are first replicated at the periphery and then move toward the inside of replication compartments,[31] somewhat similar to our observation in Ad infection. An earlier study on HCMV reported that some core histones are enriched in viral replication compartments,[32] while recent studies on herpes simplex virus-1 (HSV-1) showed rather exclusion of histones from the compartments.[33,34] As the spatial regulations for HCMV and HSV-1 genome/chromatin during progeny virion maturation remains unclear, it would be intriguing to investigate whether more viral systems have distinct early and late replication compartments and if ViPR body-like structures also exist for those viruses.

In summary, this study identified a specific late replication compartment for Ad genomes leading to the de novo formation of a novel subnuclear structure, which we termed ViPR bodies, and its molecular marker Mybbp1a. We believe that our identification of ViPR bodies as a novel compartment in the Ad infection cycle, which accumulates replicated viral genomes, and Mybbp1a as a potential host factor for these domains will help to characterize the poorly understood fate of viral progeny genomes.

4 | MATERIALS AND METHODS

4.1 | Cells and viruses

U2OS (ATCC #HTB-96) and H1299 (ATCC #CRL-5803) cells were maintained in DMEM Glutamax (Life Technologies, Carlsbad, CA, USA) supplemented with 10% of fetal calf serum (FCS). Recombinant human Ad type 5, which is genetically equivalent to the strain dl309, was amplified and purified as described previously[35,36] and used as the wildtype Ad5 virus. Ad infection was carried out at a multiplicity of infection (MOI) of 20 PFU/cell. The transfection of plasmids was done using Lipofectamine 2000 (Life Technologies) according to the manufacturer's protocol.

4.2 | Antibodies

Antibodies used in this study are as follows: rabbit anti-Mybbp1a (Abcam (Cambridge, MA, USA); ab93835, dilution 1:100 for IF, and Sigma-Aldrich (St. Louis, MO, USA); HPA005466, dilution 1:200 for WB), rat anti-protein VII (dilution 1:500 for IF, 1:1000 for WB),[4] mouse anti-protein VII (dilution 1:100 for IF),[37] mouse anti-TAF-Iβ (KM1720, dilution 1:200 for WB),[38] mouse anti-β-actin (MP Biomedicals (Santa Ana, CA, USA); dilution 1:1000 for WB), rabbit anti-histone H3 (Active motif (Carlsbad, CA, USA); 39163; dilution 1:100 for IF), rat anti-GFP (Chromotek (Planegg-Martinsried, Germany); dilution 1:1000 for WB), and Atto 488-labeled anti-GFP (GFP-Booster, Chromotek; dilution 1:200 for IF) antibodies. Rat anti-USP7 (dilution 1:30 for IF), mouse anti-DBP (dilution 1:25 for IF), and rabbit anti-hexon antibodies (dilution 1:500 for WB) were kindly provided by T. Dobner (Heinrich-Pette-Institute), R. Iggo (Institut Bergonié) and L. Gerace (Scripps Research Institute), respectively.

4.3 | Plasmids

The construction of pEGFP-C1-FLAG-Nopp140 and pcDNA3-DsRed1-FLAG-B23.1 was carried out as follows. The cDNA fragment for Nopp140 was amplified by PCR, digested with BamHI and EcoRI, and inserted into the pcDNA3.1-FLAG vector (pcDNA3.1-FLAG-Nopp140). Then the cDNA fragment for FLAG-Nopp140 was amplified by PCR, digested with BglII and EcoRI, and inserted into the pEGFP-C1 vector. The cDNA fragment for FLAG-B23.1 was released from pBS-FLAG-B23.1 by digesting with BamHI and EcoRI and then inserted into the pcDNA3 vector. The cDNA fragment for DsRed1 was amplified by PCR, digested with HindIII, and inserted into the HindIII site of the resultant vector, pcDNA3-FLAG-B23.1 (cloning details provided upon request).

The expression vectors for Mybbp1a and protein VII (pEGFP-C1-3×FLAG-Mybbp1a and pEGFP-C1-FLAG-protein VII) are generous gifts from K. Kato and M. A. Samad (University of Tsukuba), respectively. The expression vector for EGFP-FLAG-tagged B23.1 (pEGFP-C1-FLAG-B23.1) is described elsewhere.[39] The expression vector for histone H2B-tdiRFP (pCAG-H2B-tdiRFP-IP) was obtained from M.-E. Torres-Padilla's laboratory (Université de Strasbourg) via Addgene (plasmid #47884).[40]

For the preparation of cells stably expressing EGFP-3×FLAG-Mybbp1a (U2OS/E3F-Mybbp1a cells), U2OS cells were transfected with pEGFP-C1-3×FLAG-Mybbp1a and cultured in the presence of 2 mg/mL G418 for 2 weeks. Clonal selection was performed by limiting dilution.

4.4 | Indirect immunofluorescence and EdU labeling

Indirect IF analyses were carried out as described previously.[37,41,42] Briefly, cells grown on coverslips were washed with phosphate-buffered saline (PBS) and fixed with 4% EM-grade paraformaldehyde (PFA) in PBS. Then, cells were permeabilized with 0.5% Saponin in PBS and blocked with IF buffer (10% FCS and 0.2% Saponin in PBS). Primary and secondary antibodies (Alexa Fluor-labeled antibodies against mouse/rabbit/rat IgG; Life Technologies) were applied to the coverslip in IF buffer for 1 hour each. Cells were mounted in DAKO (Glostrup, Denmark) mounting media containing DAPI, and were analyzed by a Leica (Wetzlar, Germany) SP5 confocal microscope. Confocal stacks were taken every 0.3 μm, and images were processed using ImageJ (https://imagej.nih.gov/ij/) and presented as maximum intensity projections. The scale bar indicated in panels is 10 μm.

For the Click-iT EdU imaging analyses (Life Technologies), EdU was added to the culture medium at a final concentration of 10 μM at the indicated time-points. After 1 hour incubation, cells were washed with the medium and then either immediately fixed for imaging or further cultured in the absence of EdU for chasing. Cells were fixed and permeabilized as described above and subjected to Click-iT reaction with Alexa Fluor 555 azide according to the manufacturer's protocol. After the reaction, samples were extensively washed with PBS and then subjected to IF analyses as described above.

4.5 | Live-cell imaging

U2OS cells were transiently transfected with pEGFP-C1-3×FLAG-Mybbp1a and then seeded in ibidi μ-Slide VI$^{0.4}$ (Ibidi, Planegg-Martinsried, Germany). At 24 hours posttransfection (hpt), cells were either mock-infected or infected with Ad5 and cultured at 37°C. Before starting imaging, the medium was replaced by CO_2-independent medium (Life Technologies) supplemented with 10% FCS and 4 mM Glutamax (Life Technologies). Images were acquired on a Leica epifluorescence microscopy system (Leica DMI6000 B inverted microscope, HAMAMATSU (Hamamatsu, Japan) ORCA-flash2.8 digital CMO camera, 20× objective) equipped with a heated stage at 37°C. Frames were taken at 15 min intervals. Z-stacks were taken every 2.4 μm for each time-point, and the best-focused images were selected and assembled into movies using MetaMorph software, Molecular Devices, Sunnyvale, CA, USA.

4.6 | In situ PLAs

In situ PLAs were performed using Duolink In Situ PLA Fluorescence kit (Sigma-Aldrich) according to the manufacturer's protocol. For sample preparation, transiently transfected cells were used. Single images were selected displaying transfected and untransfected cells next to each other, and PLA signal intensity was determined. In order to examine the effect of the presence of transiently expressed proteins under the identical conditions, cells were analyzed in pairs.

4.7 | Western blot analyses

To prepare cell lysates, cells were resuspended in Pierce IP Lysis buffer (Thermo Scientific, Waltham, Massachusetts, USA) containing 1 mM phenylmethylsulphonyl fluoride (PMSF) and then sonicated. Lysates were subjected to SDS–PAGE, and proteins were transferred to nitrocellulose membranes (Thermo Scientific). Membranes were blocked with 5% skimmed milk/Tris-buffered saline (TBS) and then incubated with indicated primary antibodies. Primary antibodies were detected using horseradish peroxidase (HRP)-conjugated secondary antibodies (Interchim, Montluçon, FRANCE). The blots were developed using Immobilon Western Chemiluminescent HRP substrate (Millipore, Billerica, Massachusetts, USA).

4.8 | Immunoprecipitation

Cell lysates prepared as described above were mixed with GFP-Trap agarose beads (Chromotek) and incubated at 4°C for 3 hour with rotation. Then beads were washed 3× with a buffer containing 10 mM Tris–HCl [pH 7.9], 100 mM NaCl, 1 mM EDTA, 0.5% NP-40, 5% glycerol and 1 mM PMSF, and precipitates were subjected to SDS–PAGE and western blotting as described above.

4.9 | Extraction of viral DNA and quantitative PCR analyses

At indicated time-points, infected cells were collected and resuspended in fresh DMEM. To release viral particles as well as intracellular viral DNA, cell suspensions were extracted by five repeated freeze/thaw cycles. Viral DNA was extracted from the supernatant using High Pure Viral Nucleic Acid Kit (Roche, Basel, Switzerland) according to the manufacturer's protocol. The quantitative PCR (qPCR) was performed using B-R SYBR Green SuperMix for iQ (Quanta Biosciences, Beverly, MA, USA) and MyiQ Real-Time PCR System (Bio-Rad, Hercules, California, USA). The reaction condition was as follows: 5 minutes at 95°C, 40 cycles of 10 seconds at 95°C, 20 seconds at 58°C and 20 seconds at 72°C. The primers used here, AQ1 and AQ2, are targeted to the hexon gene.[43]

ACKNOWLEDGMENTS

We thank T. Dobner, R. Iggo, V. Parissi and L. Gerace for the antibodies, and K. Kato, M. A. Samad and M.-E. Torres-Padilla for the plasmids. We thank G. Längst for carefully reading the manuscript and helpful comments. The microscopy was performed in the Bordeaux Imaging Center, a service unit of the CNRS-INSERM and Bordeaux University, member of the national infrastructure France BioImaging. H.W. is an INSERM fellow.

This work was in part supported through ANR grant (ANR 14 IFEC 0003-04) Infect-ERA, project eDEVILLI (H.W.), a BIS-Japan travel grant from the Excellence Initiative (IdEX) of the Bordeaux University (T.K.) and Grants-in-aid from the Ministry of Education, Culture, Sports, Science and Technology of Japan (M.H., M.O. and K.N.).

The Editorial Process File is available in the online version of this article.

REFERENCES

1. Knipe DM, Lieberman PM, Jung JU, et al. Snapshots: chromatin control of viral infection. *Virology*. 2013;435:141–156.
2. Russell WC. Adenoviruses: update on structure and function. *J Gen Virol*. 2009;90:1–20.
3. Giberson AN, Davidson AR, Parks RJ. Chromatin structure of adenovirus DNA throughout infection. *Nucleic Acids Res*. 2012;40:2369–2376.
4. Haruki H, Gyurcsik B, Okuwaki M, Nagata K. Ternary complex formation between DNA-adenovirus core protein VII and TAF-Iβ/SET, an acidic molecular chaperone. *FEBS Lett*. 2003;555:521–527.
5. Komatsu T, Haruki H, Nagata K. Cellular and viral chromatin proteins are positive factors in the regulation of adenovirus gene expression. *Nucleic Acids Res*. 2011;39:889–901.
6. Komatsu T, Nagata K. Replication-uncoupled histone deposition during adenovirus DNA replication. *J Virol*. 2012;86:6701–6711.
7. Sergeant A, Tigges MA, Raskas HJ. Nucleosome-like structural subunits of intranuclear parental adenovirus type 2 DNA. *J Virol*. 1979;29:888–898.
8. Dery CV, Toth M, Brown M, Horvath J, Allaire S, Weber JM. The structure of adenovirus chromatin in infected cells. *J Gen Virol*. 1985;66:2671–2684.
9. Daniell E, Groff DE, Fedor MJ. Adenovirus chromatin structure at different stages of infection. *Mol Cell Biol*. 1981;1:1094–1105.
10. Ross PJ, Kennedy MA, Christou C, Risco Quiroz M, Poulin KL, Parks RJ. Assembly of helper-dependent adenovirus DNA into chromatin promotes efficient gene expression. *J Virol*. 2011;85:3950–3958.
11. Hake SB, Allis CD. Histone H3 variants and their potential role in indexing mammalian genomes: the 'H3 barcode hypothesis'. *Proc Natl Acad Sci USA*. 2006;103:6428–6435.
12. Pombo A, Ferreira J, Bridge E, Carmo-Fonseca M. Adenovirus replication and transcription sites are spatially separated in the nucleus of infected cells. *EMBO J*. 1994;13:5075–5085.
13. Ching W, Koyuncu E, Singh S, et al. A ubiquitin-specific protease possesses a decisive role for adenovirus replication and oncogene-mediated transformation. *PLoS Pathog*. 2013;9:e1003273.

14. Hasson TB, Ornelles DA, Shenk T. Adenovirus L1 52- and 55-kilodalton proteins are present within assembling virions and colocalize with nuclear structures distinct from replication centers. *J Virol*. 1992;66:6133–6142.
15. Hiscox JA, Whitehouse A, Matthews DA. Nucleolar proteomics and viral infection. *Proteomics*. 2010;10:4077–4086.
16. Greco A. Involvement of the nucleolus in replication of human viruses. *Rev Med Virol*. 2009;19:201–214.
17. Samad MA, Komatsu T, Okuwaki M, Nagata K. B23/nucleophosmin is involved in regulation of adenovirus chromatin structure at late infection stages, but not in virus replication and transcription. *J Gen Virol*. 2012;93:1328–1338.
18. Samad MA, Okuwaki M, Haruki H, Nagata K. Physical and functional interaction between a nucleolar protein nucleophosmin/B23 and adenovirus basic core proteins. *FEBS Lett*. 2007;581:3283–3288.
19. Ugai H, Dobbins GC, Wang M, Le LP, Matthews DA, Curiel DT. Adenoviral protein V promotes a process of viral assembly through nucleophosmin 1. *Virology*. 2012;432:283–295.
20. Lam YW, Evans VC, Heesom KJ, Lamond AI, Matthews DA. Proteomics analysis of the nucleolus in adenovirus-infected cells. *Mol Cell Proteomics*. 2010;9:117–130.
21. Hochstatter J, Hölzel M, Rohrmoser M, et al. Myb-binding protein 1a (Mybbp1a) regulates levels and processing of pre-ribosomal RNA. *J Biol Chem*. 2012;287:24365–24377.
22. Tan BC-M, Yang C-C, Hsieh C-L, et al. Epigeneitc silencing of ribosomal RNA genes by Mybbp1a. *J Biomed Sci*. 2012;19:57.
23. Mori S, Bernardi R, Laurent A, et al. Myb-binding protein 1A (MYBBP1A) is essential for early embryonic development, controls cell cycle and mitosis, and acts as a tumor suppressor. *PLoS One*. 2012;7:e39723.
24. Kuroda T, Murayama A, Katagiri N, et al. RNA content in the nucleolus alters p53 acetylation via MYBBP1A. *EMBO J*. 2011;30:1054–1066.
25. Hindley CE, Davidson AD, Matthews DA. Relationship between adenovirus DNA replication proteins and nucleolar proteins B23.1 and B23.2. *J Gen Virol*. 2007;88:3244–3248.
26. Wang I-H, Suomalainen M, Andriasyan V, et al. Tracking viral genomes in host cells at single-molecule resolution. *Cell Host Microbe*. 2013;14:468–480.
27. Gyurcsik B, Haruki H, Takahashi T, Mihara H, Nagata K. Binding modes of the precursor of adenovirus major core protein VII to DNA and template activating factor I: implication for the mechanism of remodeling of the adenovirus chromatin. *Biochemistry*. 2006;45:303–313.
28. Komatsu T, Sekiya T, Nagata K. DNA replication-dependent binding of CTCF plays a critical role in adenovirus genome functions. *Sci Rep*. 2013;3:2187.
29. Yamauchi T, Keough RA, Gonda TJ, Ishii S. Ribosomal stress induces processing of Mybbp1a and its translocation from the nucleolus to the nucleoplasm. *Genes Cells*. 2008;13:27–39.
30. Cavellán E, Asp P, Percipalle P, Farrants A-KO. The WSTF-SNF2h chromatin remodeling complex interacts with several nuclear proteins in transcription. *J Biol Chem*. 2006;281:16264–16271.
31. Strang BL, Boulant S, Chang L, Knipe DM, Kirchhausen T, Coen DM. Human cytomegalovirus UL44 concentrates at the periphery of replication compartments, the site of viral DNA synthesis. *J Virol*. 2012;86:2089–2095.
32. Nitzsche A, Paulus C, Nevels M. Temporal dynamics of cytomegalovirus chromatin assembly in productively infected human cells. *J Virol*. 2008;82:11167–11180.
33. Dembowski JA, DeLuca NA. Selective recruitment of nuclear factors to productively replicating herpes simplex virus genomes. *PLoS Pathog*. 2015;11:e1004939.
34. Lang F-C, Li X, Vladmirova O, et al. Selective recruitment of host factors by HSV-1 replication centers. *Zool Res*. 2015;36:142–151.
35. Schreiner S, Martinez R, Groitl P, et al. Transcriptional activation of the adenoviral genome is mediated by capsid protein VI. *PLoS Pathog*. 2012;8:e1002549.
36. Wodrich H, Henaff D, Jammart B, et al. A capsid-encoded PPxY-motif facilitates adenovirus entry. *PLoS Pathog*. 2010;6:e1000808.
37. Komatsu T, Dacheux D, Kreppel F, Nagata K, Wodrich H. A method for visualization of incoming adenovirus chromatin complexes in fixed and living cells. *PLoS One*. 2015;10:e0137102.
38. Nagata K, Saito S, Okuwaki M, et al. Cellular localization and expression of template-activating factor I in different cell types. *Exp Cell Res*. 1998;281:274–281.
39. Hisaoka M, Ueshima S, Murano K, Nagata K, Okuwaki M. Regulation of nucleolar chromatin by B23/nucleophosmin jointly depends upon its RNA binding activity and transcription factor UBF. *Mol Cell Biol*. 2010;30:4952–4964.
40. Miyanari Y, Ziegler-Birling C, Torres-Padilla M-E. Live visualization of chromatin dynamics with fluorescent TALEs. *Nat Struct Mol Biol*. 2013;20:1321–1324.
41. Komatsu T, Nagata K, Wodrich H. An adenovirus DNA replication factor, but not incoming genome complexes, targets PML nuclear bodies. *J Virol*. 2016;90:1657–1667.
42. Komatsu T, Will H, Nagata K, Wodrich H. Imaging analysis of nuclear antiviral factors through direct detection of incoming adenovirus genome complexes. *Biochem Biophys Res Commun*. 2016;473:200–205.
43. Heim A, Ebnet C, Harste G, Pring-Akerblom P. Rapid and quantitative detection of human adenovirus DNA by real-time PCR. *J Med Virol*. 2003;70:228–239.

SUPPORTING INFORMATION

Additional Supporting Information may be found online in the supporting information tab for this article.

How to cite this article: Komatsu T, Robinson DR, Hisaoka M, Ueshima S, Okuwaki M, Nagata K, Wodrich W. Tracking adenovirus genomes identifies morphologically distinct late DNA replication compartments, *Traffic*, 2016;17(11):1168–1180.